GEOPHYSICAL RESEARCH LETTERS, VOL. 26, NO. 14, PAGES 2109-2112, JULY 15, 1999

From diffuse to localised damage through elastic interaction

David AMITRANO
Lirigm, Université Joseph Fourier, Grenoble, France

Jean-Robert GRASSO
LGIT, Observatoire de Grenoble, France

Didier HANTZ
Lirigm, Université Joseph Fourier, Grenoble, France

Abstract. Local damage processes that have been reported for ductile and brittle macroscopic behaviours are shown here to provide a possible link between these two contrasting behaviours. Using a local progressive damage law within a linear tensorial elastic interaction model, we reproduce experimentally observed macroscopic non-linear behaviours that continuously range from ductility with diffuse damage to brittleness with localised damage. The model exhibits power law distributions of damage events in space and size domains. The diffuse-localised and induced ductile-brittle transition appear to be controlled by the internal friction angle which influences the local interaction geometry.

Introduction

The mechanical response of rock materials to loading involves damage processes including fracturing which involves acoustic wave emission (AE) [*Lockner*, 1993]. For brittle materials, the failure occurs due to cooperative interaction of microruptures, i.e. damage localisation, that is experimentally observed by AE source location [e.g. *Lockner et al.*, 1991]. Ductile behaviour, associated with diffuse damage [*Hirata et al.*, 1987], can be obtained for the same materials, by changing the loading conditions (e.g. increasing confining pressure). It suggests a continuous transition from diffuse to localised damage. In all cases, the AE event distributions, in size and space domain, are reported to exhibit power law behaviour [*Hirata et al.*, 1987; *Lockner*, 1993] arguing for long range correlations. Using local progressive damage and elastic interaction, previous attempts succeeded in modelling either macroscopic plasticity (scalar model, *Zapperi et al.* [1997]) or macroscopic brittleness (tensorial model, *Tang* [1997]).

In the presented model, using a local scalar damage formulation associated with a tensorial elastic interaction model, we succeed in switching continuously from macroscopic plasticity, with diffuse damage, to macroscopic brittleness, with localised damage.

Description of the progressive damage model

Damage is usually modelled as the change of material elastic properties induced by defects. From an observational point of view, AE is used as a relevant tool to monitor the crack nucleation and growth, i.e. damage increase, in space, size, and time domains [*Cox and Meredith*, 1993; *Hirata et al.*, 1987; *Lockner*, 1993]. In the case of rocks, damage has been proposed to be related to crack density [*Kemeny and Cook*, 1986]. In order to quantitatively describe damage increase, we use a scalar relationship between the elastic modulus of a reference material and the damaged material, E and $\tilde{E}$ respectively, assuming an isotropic damage.

$$\tilde{E} = (1 - D)E \tag{1}$$

where D is the damage. Such a relation works when the studied volume is large compared with the defect size. According to *Kemeny and Cook* [1986] the Poisson's ratio ν should be corrected for the damage. Tests have shown that this feature has no effect on our modelling results. Consequently we use constant Poisson ratio for all the simulations.

The elastic simulated material, defined by E and the Poisson ratio ν, is discretized using a finite element method to calculate the stress state in each element due to the loading of the model. Following *Zapperi et al.* [1997], we assume that each element corresponds to a mesoscopic scale, i.e. the defect size is small compared with the element size. As we focus on geomaterials, we choose the tensorial Mohr-Coulomb criterion (F) as a damage threshold.

$$F = (C + \sigma \tan\phi) - \tau \tag{2}$$

where τ is the shear stress, σ the normal stress, C the cohesion and ϕ, the internal friction angle. Mohr assumed that the plane which fulfils the criterion is the potential fracture plane. Here we use this criterion as an isotropic damage threshold.

To simulate material heterogeneity we classically use an initial element cohesion C that is randomly drawn from a uniform distribution [*Herrmann and Roux*, 1990; *Zapperi et al.*, 1997]). The other parameters (E, ν, ϕ) are initially constant for all the elements. The same results are obtained using a frozen cohesion and an initially random elastic modulus. For each element, each time the stress exceeds the criterion (2), the damage increases locally using relation (1), i.e. E is decreased by a factor (1-D), D being constant [*Zapperi et al.*, 1997]. Moreover a new cohesion is redrawn from the initial distribution to simulate the material heterogeneous strength during the damage increase.

To reduce computation delays the simulation is performed on a 2D plane strain FEM model, using three node isoscele triangular mesh. The same mesh is used along the simulation.

Paper number 1999GL900388.
0094-8276/99/1999GL900388$05.00

The precision is about 10^{-4} and the residue about 10^{-12}. The loading consists of progressively increasing the vertical displacement of the upper boundary, the lower being kept fixed, as is generally done during laboratory tests. A confining pressure is applied on lateral boundaries to simulate triaxial stress conditions.

When an element reaches its damage threshold, it is damaged as described previously. Because of the elastic interaction, the stress redistribution around a damaged element can induce an avalanche of damage. For the same loading step, we compute the stress state until every element is below the damage threshold. The total number of damage events during a single loading step is the avalanche size.

To quantitatively estimate the damage clustering, i.e. localisation, we calculate the correlation dimension (*D2*) of the damaged elements using the box-counting method [e.g. *Cowie et al.*, 1995].

Results

Our tensorial model combines ingredients of models that either reproduce macroscopic ductility [*Zapperi et al.*, 1997] or brittleness [*Tang*, 1997], one remaining parameter being free, i.e. ϕ the internal friction angle. As ϕ characterises the confining pressure sensitivity, we performed simulations with various confining pressures [*Amitrano*, 1999].

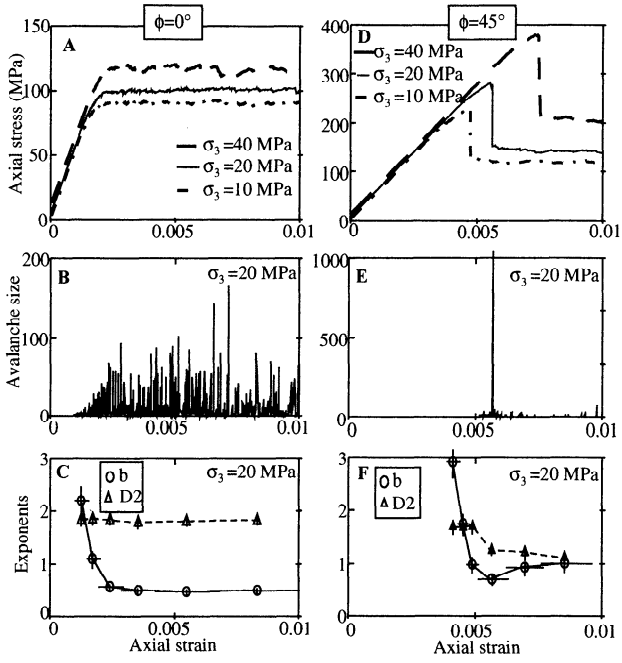

Figure 1. Simulated macroscopic behaviour for ϕ=0° (A-B-C) and ϕ=45° (D-E-F). The other model parameters are constant: $E_{initial}$=50 GPa, ν=0.25, C = randomly drawn between 25 and 50 MPa, D = 0.05. A-D : Macroscopic strain-stress curves for confining pressure, σ_3, ranging from 10 to 40 MPa. B-E: Avalanche activity versus strain for σ_3 = 20 MPa. C-D : Size and space exponents (b and $D2$ respectively) calculated for successive windows containing equal numbers of avalanches. The horizontal bars indicate the period covered by the calculated exponent, the vertical bars give the estimation error for a confidence level of 95%. Several values of D have been tested. This parameter only influences the number of avalanches during a simulation. The model size is 540 elements.

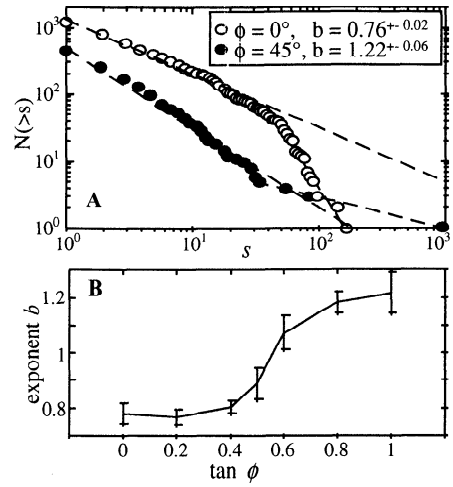

Figure 2. A: Cumulative distributions of avalanche sizes, s. Each distribution includes the entire simulated population for ϕ=0 (open circles) and ϕ=45° (black circles) respectively. B: Exponent b calculated for each entire simulation as a function of ϕ. The vertical bars give the estimation error for a confidence level of 95%. The exponent is calculated for the linear part of each distribution.

Here we present results obtained for two extreme values of this parameter (ϕ=0° as observed for ductile materials, i.e. ice, and ϕ=45° as observed for brittle materials, i.e. granite at low confining pressure) and for confining pressure ranging from 10 to 40 MPa. The other parameters are kept fixed.

Fig. 1A shows macroscopic stress-strain curves for ϕ=0°. Changes in confining pressure just change the maximal strength. It does not modify the macroscopic behaviour which always remains ductile. The simulated avalanche activity is associated with the so-called macroscopic plastic stage (Fig. 1B) as observed for AE monitoring during laboratory tests on ice [*Weiss and Grasso*, 1997]. The simulated avalanche sizes display a power law distribution with a cut-off corresponding to a finite size effect (Fig. 2A). In order to explore the temporal variations of damage, we computed the exponent of the power law distributions in size and space domains, i.e. b and $D2$, for successive windows of equal avalanches number (Fig. 1C). The value for b starts decreasing from above 2 to less than 1 and stabilises when the steady (plastic) stage is reached. $D2$ remains roughly close to 2 which corresponds to diffuse damage that almost completely fills the space (Fig. 3A). Such a pattern is recurrently observed for all the tested confining pressures.

Fig. 1(D-E-F) shows results for ϕ=45°. The macroscopic behaviour displays brittleness, i.e. macroscopic instability, that occurs after elastic behaviour and before plastic steady behaviour (Fig. 1D-E). The avalanche size still displays power-law distribution except for the larger event which corresponds to the macrorupture (Fig. 2A). The b pattern for successive windows displays a minimum value before the macrorupture, as classically reported for laboratory tests [e.g. *Lockner*, 1993; *Main et al.*, 1989; *Scholz*, 1968]. The progressive damage localisation, expressed by the decrease of $D2$ from a value close to 2 (diffuse within a plane) to a value close to 1 (localised along a line) is shown on Fig. 3B. Such a $D2$ decrease agrees with laboratory AE location observation on brittle rocks [*Lockner*, 1993]. Note that macroscopic strain

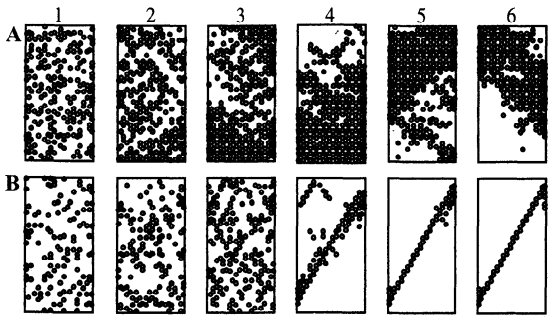

Figure 3. Damage evolution during simulation for ϕ=0° (A) and for ϕ=45° (B). Each map (1-6) shows the newly damaged elements during successive simulation steps containing an equal number of damage avalanches as shown in Fig. 1C and 1F. For (A) the lattice geometry doesn't change the behaviour. For (B) the damage directions that result from ϕ change are also affected by the lattice directions. Tests of the impact of the size and the aspect ratio of the mesh have shown no effect on the behaviour [*Amitrano*, 1999].

softening (Fig. 1D) is obtained without including local strain softening, contrary to the model of *Tang* [1997].

Such a pattern is recurrently observed for all the tested confining pressure values, including zero. We did not observed the « axial splitting » typical of the uniaxial loading, which is induced by tensile failure. In our model no tensile criterion is used. As ϕ also influences the maximal macroscopic strength, we performed simulations with enlarged C values for ϕ=0° in order to obtain the same strength value than for ϕ=45°. We recover the same results than the ones presented on the Fig. 1-3.

These results argue for the difference between diffuse and localised damage to be related to internal friction ϕ rather than to the confining pressure or the maximal strength.

Discussion

By tuning the single ϕ parameter, our model allows us to simulate macroscopic behaviours that range from ductility with diffuse damage (ϕ=0°) to brittleness with localised damage (ϕ=45°).

It has been documented in experimental studies that materials with large internal friction angle tend to fail by localised failure when loaded in triaxial compression, whereas those with very low internal friction angle fail by a diffuse mode [*Jaeger and Cook*, 1979]. Moreover, the apparent internal friction angle (inferred from the slope of the Mohr envelope) is experimentally reported to decrease with increasing confining pressure [e.g. *Hoek and Brown*, 1982]. Contemporary to confining pressure increase the macroscopic behaviour becomes more ductile and the damage more diffuse [*Ayling et al.*, 1995; *Brady and Brown*, 1993; *Velde et al.*, 1993].

The presented model allows us to simulate these well established observations by tuning the ϕ parameter (Fig. 1). The Mohr-Coulomb criterion we used is linear, i.e. the slope of the Mohr envelope is constant and does not depend on the confining pressure. It allows us to uncouple the effect of internal friction angle (Mohr envelope slope) from those of confining pressure. Our results argue for the difference between diffuse and localised damage to be solely related to internal friction ϕ. Consequently the localised-diffuse damage transition and the associated brittle-ductile transition appears to be driven by the decrease of the internal friction angle ϕ. Note that when using an empirical criterion where ϕ is pressure dependent [*Hoek and Brown*, 1982], we recover the observed macroscopic brittle-ductile transition induced by confining pressure increase [*Amitrano*, 1999].

In order to understand why changes on ϕ lead to changes in the macroscopic behaviour, we study the effect of ϕ on the Mohr-Coulomb criterion (F in eq. 2) field around a single isotropic defect. Fig. 4 shows interrelation between ϕ and the geometry of the F field as the damage increases. For low ϕ value the surrounding F field shows low gradient that allows interaction with other defects in any direction (diffuse interaction). On the contrary a high ϕ value leads to a F field with a strong directionality and a strong gradient that both increase as damage progresses, restricting the possible interaction domain (localised interaction).

For each defect ϕ controls the surrounding F field perturbation and thus the nature of interaction. Consequently the local interaction geometry driven by ϕ controls the macroscopic localisation mode (Fig. 3A-B).

The change of local interaction geometry, through ϕ change, also influences the avalanche dynamics as expressed by the change in the b exponent (Fig. 2A-B). The simulated b values increase when switching from macroscopic ductility to brittleness (Fig. 2 A-B). This agrees with the negative correlation between b and the confining pressure observed during laboratory tests [*Amitrano and Hantz*, 1998] and with the reported depth dependence of frequency-magnitude distribution of earthquakes [e.g. *Mori and Abercombie*, 1997].

One remaining question is why (how) does increased confining pressure cause a change in the apparent value of the internal friction angle. Classically ϕ is used as an index of the confining pressure dependence of the material strength that empirically allows to recover a wide range of macroscopic behaviours. One way to highlight a physical meaning for ϕ may be found out considering the competition between two

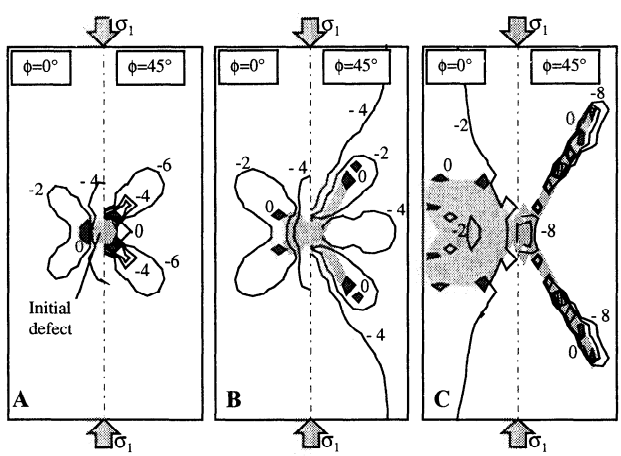

Figure 4. A map of the F criterion field around a single pre-damaged defect ($E_{defect.}$ = 25 GPa) into an homogeneous material ($E_{material}$ = 50 GPa), obtained with ϕ=0° (left part) and ϕ=45° (right part) respectively. The simulations was performed by increasing vertical strain and stopped at three different steps of damage propagation (A, B, C). Negative values indicate the criterion is not reached. The Dark areas indicate the zero F value, i.e. the damage process zone. The shaded areas indicate the damaged element.

processes, crack/dislocation propagation, associated with two end member behaviours, brittleness/plasticity.

The dislocation propagation involved in plasticity depends only on the applied shear stress as expressed by the plasticity Tresca criterion where ϕ=0°. On the other hand, crack propagation, as considered in the Griffith theory, occurs when the tensile strength at the crack tip is reached. Consequently crack propagation depends on the confining pressure, what corresponds to $\phi > 0$. The coexistence of these two processes during brittle-ductile transition has been experimentally observed [e.g. *Darot et al.*, 1985].

The confining pressure increase closes the cracks which impedes their propagation but has no effect on dislocation propagation [*Guéguen and Palciauskas*, 1992]. As the confining pressure increases the crack process is progressively replaced by the dislocation process, that leads to a ϕ decrease.

Note that if the competition between dislocation and cracks to accommodate deformation appears as a possible physical meaning for ϕ change, it does not agree with the damage rules of our model. We choose to relax stress by decreasing Young's modulus that is relevant for crack but irrelevant for dislocation process. An alternative for stress relaxation could be to include in simulations a local increase of the permanent deformation.

Nevertheless our model provides a novel explanation for a phenomenon observed on rock deformation experiment which has previously only been described : the localised-diffuse transition associated to the brittle-ductile transition due to increased confining pressure.

Conclusion

Our model shows how a simple local damage rule can induces a broad type of macroscopic behaviours ranging from ductility with diffuse damage to brittleness with localised damage. Simulation results allow us to propose the control parameter of the diffuse-localised damage transition to be the internal friction angle of the Mohr-Coulomb criterion. This parameter controls the local interaction geometry between defects and then the macroscopic damage distribution type, diffuse/localised. The ductile-brittle macroscopic behaviour appears as a consequence of the progressive localisation of damage.

The physical meaning of the internal friction angle is not yet obvious and particularly its dependence on the confining pressure. We suggest this parameter to decrease as elementary processes switch from crack propagation to dislocation propagation when the confining pressure increase.

Acknowledgements. This research was supported by FORPRO-ANDRA, PNRN-INSU and PGRN programs. The authors thank A.M. Boullier, F. Lahaie, J. Weiss and two anonymous reviewers for constructive comments.

References

Amitrano, D. (1999) Emission acoustique des roches et endommagement: Approches expérimentale et numérique, Application à la sismicité minière. PhD Thesis, p. 250. Université Joseph Fourier, Grenoble, France.

Amitrano, D., and D. Hantz, Acoustic emission of jointed and intact rocks during triaxial compression test, in *Int. Conf. on Mechanics of Jointed and Faulted Rock*, pp. 375-380, Vienna, 1998.

Ayling, M.R., P.G. Meredith, and S.A.F. Murrell, Microcracking during triaxial deformation of porous rocks monitored by changes in rock physical properties, I. Elastic wave propagation measurments on dry rocks, *Tectonophys., 245*, 205-221, 1995.

Brady, B.H.G., and E.T. Brown, *Rock mechanics for underground mining*, 569 pp., Chapman & Hall, 1993.

Cowie, P.A., D. Sornette, and C. Vanneste, Multifractal scaling properties of a growing fault population, *Geophys. J. Int., 122*, 457-469, 1995.

Cox, S.J.D., and P.G. Meredith, Microcrack formation and material softening in rock measured by monitoring acoustic emission, *Int. J. Rock Mech. Min. Sci. & Geomech. Abstr., 30 (1)*, 11-24, 1993.

Darot, M., Gueguen, Y., and Bencheman, Z. (1985) Ductile-brittle transition investigated by micro-indentation : results for quartz and olivine. *Phys. Earth and Plan. Int., 40*, 180-186.

Guéguen, Y., and Palciauskas, V. (1992) *Introduction à la physique des roches*. 299 p. Hermann, Paris.

Herrmann, H.J., and S. Roux, *Statistical models for the fracture of disordered media*, 353 pp., North-Holland, Amsterdam, 1990.

Hirata, T., T. Satoh, and K. Ito, Fractal structure of spacial distribution of microfracturing in rock, *Geophys. J. R. astr. Soc., 90*, 369-374, 1987.

Hoek, E., and Brown, E.T. (1982) *Underground excavations in rock*. 527 p. Institution of Mining and Metallurgy, London.

Jaeger, J.C., and N.G.W. Cook, *Fundamentals of rock mechanics*, 593 pp., Chapman & Hall, London, 1979.

Kemeny, J., and N.G.W. Cook, Effective moduli, Non-linear deformation and strength of a cracked elastic solid, *Int. J. Rock Mech. Min. Sci. & Geomech. Abstr., 23 (2)*, 107-118, 1986.

Lockner, D.A., The role of acoustic emission in the study of rock fracture, *Int. J. Rock Mech. Min. Sci. & Geomech. Abstr., 30 (7)*, 883-899, 1993.

Lockner, D.A., J.D. Byerlee, V. Kuskenko, A. Ponomarev, and A. Sidorin, Quasi-static fault growth and shear fracture energy in granite, *Nature, 350*, 39-42, 1991.

Main, I.G., P.G. Meredith, and C. Jones, A reinterpretation of the precursory seismic b-value anomaly from fracture mechanics, *Geophys. J., 96*, 131-138, 1989.

Mori, J., and R.E. Abercombie, Depth dependence of earthquake frequency-magnitude distributions in California: Implication for rupture initiation, *J. Geophys. Res., 102 (B7)*, 15081-15090, 1997.

Scholz, C.H., The frequency-magnitude relation of microfracturing in rock and its relation to earthquakes, *Bull. Seismol. Soc. Am., 58 (1)*, 399-415, 1968.

Tang, C.A., Numerical simulation of progressive rock failure and associated seismicity, *Int. J. Rock Mech. Min. Sci. & Geomech. Abstr.*, 34 (2), 249-261, 1997.

Velde, B., D. Moore, A. Badri, and B. Ledesert, Fractal analysis of fractures during brittle to ductile changes, *J. Geophys. Res., 98 (B7)*, 11935-11940, 1993.

Weiss, J., and J.R. Grasso, Acoustic emission in single crystals of ice., *J. Phys. Chem., 101*, 6113-6117, 1997.

Zapperi, S., A. Vespignani, and E. Stanley, Plasticity and avalanche behaviour in microfracturing phenomena, *Nature*, 388 (14 august 1997), 658-660, 1997.

D. Amitrano, D. Hantz, LIRIGM, Université Joseph Fourier, BP 53, Grenoble Cedex 9, France. (e-mail: david.amitrano@ujf-grenoble.fr, didier.hantz@ujf-grenoble.fr

J-R. Grasso, LGIT, Observatoire de Grenoble, BP 53, Grenoble Cedex 9, France. (e-mail: grasso@lgit.obs.ujf-grenoble.fr)

(Received November 3, 1998; revised: march 5, 1999; accepted march 23, 1999)